Am J Transl Res 2021;13(4):2111-2126
www.ajtr.org /ISSN:1943-8141/AJTR0117709

Original Article

NEAT1 promotes the repair of abdominal aortic aneurysms of endothelial progenitor cells via regulating miR-204-5p/Ang-1

Chao Shi[1], Chongwen Shen[1], Ge Liu[1], Shaofeng Yang[1], Fenglin Ye[1], Jinjin Meng[1], Youmin Pan[2]

[1]*Department of Cardiothoracic Surgery, The First Affiliated Hospital of Bengbu Medical College, Bengbu, China;* [2]*Department of Cardiovascular Surgery, Tongji Hospital, Tongji Medical College, Huazhong University of Science and Technology, Wuhan 430030, Hubei Province, China*

Received July 7, 2020; Accepted December 26, 2020; Epub April 15, 2021; Published April 30, 2021

Abstract: Purpose: To clarify the regulatory effect of Nuclear-enriched abundant transcript 1 (NEAT1) on abdominal aortic aneurysm (AAA) model rats and isolated endothelial progenitor cells (EPCs). Methods: The AAA rat model was established by $CaCl_2$ stimulation, and overexpressed NEAT1 was injected into rats through tail vein. Abdominal aorta lesions and numbers of EPCs in tissues and peripheral blood were examined by hematoxylin-eosin, immunofluorescence and flow cytometry. The extracted EPCs were identified by microscopy, DiI-ac-LDL staining and flow cytometry. Effect of overexpressed/silencing NEAT1 on the viability, migration, tube formation and VEGF content of EPCs was investigated by MTT-, wound-healing, tube formation assays and ELISA, respectively. The expressions of NEAT1, miR-204-5p, Angiopoietin-1 (Ang-1)/ERK pathway were determined by qRT-PCR and Western blot as needed. The targeting relationships between NEAT1 and miR-204-5p, and miR-204-5p and Ang-1 were predicted on starBase, TargetScan and confirmed by dual-luciferase experiments. The mutual regulation effect was studied through rescue experiments. Results: Overexpressed NEAT1 not only reduced inflammatory infiltration and increased the number of EPCs in abdominal aorta and peripheral blood, but also promoted the viability, migration, tube formation of EPCs, increased VEGF content and upregulated the expression of the Ang-1/ERK pathway in EPCs. However, silencing NEAT1 produced opposite results. NEAT1 targeting miR-204-5p inhibited the functional effects of miR-204-5p on of EPCs. Overexpressed/silencing Ang-1 partially reversed the effects of NEAT1 or miR-204-5p on the characteristics of EPCs. Conclusion: NEAT1 competitively binds with miR-204-5p and up-regulates Ang-1 expression in EPCs to effectively improve the proliferation, migration and angiogenesis of EPCs.

Keywords: Nuclear-enriched abundant transcript 1, abdominal aortic aneurysm, endothelial progenitor cells, miR-204-5p, Angiopoietin-1

Introduction

Abdominal aortic aneurysm (AAA) is a common aortic disease requiring vascular surgery. The mortality rate of AAA patients with aneurysm rupture exceeds 80% [1, 2]. Abdominal aortic aneurysms could be caused by atherosclerosis as well as other factors such as trauma and genetic susceptibility [3]. The incidence of abdominal aortic aneurysms is increasing annually in China [4]. At present, the main treatment of abdominal aortic aneurysms is surgery, with drug treatment as an adjuvant therapy to slow down the expansion of aneurysms [5]. However, the effect of these treatments is seriously affected by poor prognostic factors such as postoperative infection, recurrence, and stent graft occlusion [5, 6]. Therefore, developing more reliable methods for treating AAA has become an important research direction of AAA prevention and treatment in clinical practice.

In 1997, by using immunomagnetic beads, Asahara discovered that the precursor cells were able to differentiate into endothelial cells from circulating peripheral blood, and named them endothelial progenitor cells (EPCs) [7]. EPCs are critically involved in angiogenesis in the embryonic period [8]. Under physiological conditions, EPCs mainly exist in a dormant state in the bone marrow, but under infection, stress or local tissue ischemia and hypoxia,

EPCs are activated, and some vascular factors, such as vascular endothelial growth factor (VEGF), basic fibroblast growth factor (bFGF), and Nitric Oxide (NO), will be increased [9, 10]. With the action of the above vascular factors, EPCs enter the peripheral blood from the bone marrow and then transfer to the damaged site to promote the regeneration of endothelium and blood vessels, thus actively participating in local angiogenesis and endothelial cell renewal [11]. This biological feature of EPCs has currently been increasingly studied in relation to aneurysms and other vascular diseases through basic and clinical researches.

The success of monoclonal antibody drugs such as VEGF and CD20 in the treatment of malignant tumors provides an important reference for the application of the molecular targeted therapy to refractory diseases [12]. Noncoding RNAs are key targets in research on the molecular targeted therapy. LncRNA nuclear-enriched abundant transcript 1 (NEAT1) is located at the nucleus and participates in the regulation of the core structure constituting the paranuclear plaque and the transcription of many genes [13]. NEAT1 has been reported to be abnormally expressed in many human malignant tumors, such as in glioma, non-small cell carcinoma, and breast cancer [14]. By studying undifferentiated human embryonic stem cells, Chen [15] found that loss of NEAT1 affects the fate of human embryonic stem cells. Abu Shufian Ishtiaq Ahmed [16] observed that NEAT1 could inhibit the expressions of smooth muscle contraction-related proteins by regulating epigenetic mechanisms, and therefore, he believed that NEAT1 could be used as a molecular target for treating occlusive vascular diseases. Based on the above findings, we hypothesized that NEAT1 may interfere with the AAA repair process of endothelial progenitor cells.

In this study, the AAA rat model and isolated induced EPCs were used as the research objects. The specific role and mechanism of NEAT1 in the AAA repair process involving EPCs were explored by performing *in vivo* and *in vitro* experiments.

Methods

Ethics statement

Animal experiments were conducted under the approval of the Animal Experiment Ethics Committee of the First Affiliated Hospital of Bengbu Medical College (201911047XGWK) and under the guidance of Guide for the Care and Use of Laboratory Animals. The SD male rats (age: 6 weeks old, weight: about 200 g) used in the experiment were purchased from Jiangsu ALF Biotechnology Co., Ltd. The feeding and experimental environment (day/night cycle with 12 hours of light, 20 ± 2°C, and 55 ± 5% humidity) was determined at the animal center of The First Affiliated Hospital of Bengbu Medical College.

Construction and transfection of NEAT1 lentiviral plasmid

The full-length sequence of NEAT1 was amplified for the construction of the overexpressed NEAT1 plasmid. After being processed with restriction enzymes (Not I, 1166S, 1094S, TAKARA, China; XhoI, 1094S, TAKARA, China) and T4 DNA Ligase (EL0011, ThermoFisher, USA), the amplified sequences were ligated into pLL3.7 lentiviral vector (VT2204, YouBio, China). SiNEAT (knocked down NEAT1, target sequence: 5'-CTCTAGGTTTGGCGCTAAACTCT-3') with a stem-loop structure was inserted to the pGLVU6/GFP vector (C06001, GenePharma, China).

The recombinant plasmids were added to DH5α competent cells (ML-G2016, Mlbio, China) and LB medium (LB-01, Coolaber, China). After 45 minutes of resuscitation, 200 μL of cells were transferred to Ampicillin LB plates (Coolaber, China) and evenly coated. The inverted plate was cultured in a cell incubator at 37°C (QP-80S, BIOBASE, China) for 16 h. Subsequently, a plasmid mini-prep kit (AP-MN-P-250G, Axygen, USA) was used for positive clone sequencing on the cloned colonies. Then plasmids were extracted from the clone colonies and further reacted with the plasmid extraction kit (AP-MX-P-25G, Axygen, USA). Afterwards, the extracted plasmids were transfect into 293T cells (CL-0005, Procell, China) using a Lipofectamine 2000 Transfection Kit (11668500, ThermoFisher, USA). 48 h after transfection, the supernatant of cells transfected with overexpressed NEAT1/siNEAT was collected. The negative control (NC) of overexpressed NEAT1 was transfected with empty pLL3.7 vector into cells, while the negative control (siNC) of siNEAT1 was transfected with empty pCDH-CMV-MCS-EF1-Puro vector in the same way.

According to our experimental design, overexpressed NEAT1, siNEAT, miR-204-5p mimic (miR10000877-1-5, RIBOBIO, China), overexpressed Ang-1 (CAT #: RR212791, ORIGENE, USA) and knocked down Ang-1 (CAT #: SR512502, ORIGENE, USA) were used to process the cells. The MiR-204-5p mimic, overexpressed Ang-1 and knocked down Ang-1 were transfected into cells using Lipofectamine 2000 transfection reagent. Cells transfected with overexpressed NEAT1 and siNEAT were directly infected with the 293T cell supernatant (3 times, 4 hours/time).

Construction of rat abdominal aortic aneurysm (AAA) model

Following a previous study [17], the modeling method of $CaCl_2$ was applied to stimulate the abdominal aorta. The SD rats were divided into 4 groups (n = 10) according to the principle of random control: Sham group, Model group, Negative control (NC) group, and overexpressed NEAT1 (NEAT1) group. The rats were anesthetized by intraperitoneal injection of 1% pentobarbital sodium (P3761-25G, Sigma, USA; injection dose of 100 mg/kg). Gauze (about 1 cm^2) was pre-soaked in $CaCl_2$ solution (0.5 mol/L) or saline. The rats were fixed in the supine position with the abdomen fully exposed. A pair of surgical scissors was used to cut along the midline of the abdomen and separate the abdominal aorta between the renal artery and the iliac artery. In all groups except for the Sham group (gauze with saline), the exposed abdominal aorta was stimulated for 15 min with the gauze covered in $CaCl_2$ solution. Then the gauze in the abdominal cavity of the rat was removed and washed with saline twice to 3 times. After that, the wound was sutured layer by layer. The supernatant of cell transfected with overexpressed NEAT1 was injected into the rats of the NEAT1 group (0.2 mL) via tail-vein injection, while the cell supernatant in the NC group was replaced by empty plasmid.

On the 29th postoperative day, all the rats were anesthetized and fixed with pentobarbital sodium. After opening the abdomen, 5 mL of blood was collected from the abdominal aorta using the EDTA anticoagulation tube. The abdominal aorta was then separated and removed. Then after removing the fatty tissues from the surface of the abdominal aorta, the abdominal aorta was rinsed with cold saline and fixed in paraformaldehyde.

Pathological testing

Hematoxylin-eosin (H&E) staining was performed for observing tissue lesions. The cytoplasm was stained red with eosin, while the nucleus was stained blue with hematoxylin. In brief, the abdominal aorta in paraformaldehyde was removed and embedded into paraffin. Then 5-μm thick paraffin sections were first dewaxed and hydrated before staining by an H&E staining kit (G1120-3×100 ml, Solarbio, China). Briefly, the tissue sections were immersed in hematoxylin (10 min), differentiation solution (30 seconds), and tap water (15 min) and eosin reagent (1 min). All the experimental operations were conducted at normal temperature. Next, after dehydration, clearing, and mounting, pathological changes of the abdominal aortic tissue sections were observed under a microscope (DM1000, Leica, Germany) at 200× magnification.

Immunofluorescence staining

Von Willebrand Factor (vWF) and kinase domain containing receptor (KDR) are important relevant factors for vascular growth, thus, the changes in the number of vWF^+ and KDR^+ cells from aortic aneurysm tissues were detected by immunofluorescence staining. Briefly, the cells were permeated in 0.1% Triton™ X-100 (01-0041-00, Merck millipore, Germany) for 15 min. Endogenous peroxidase activity was blocked by with 3% H_2O_2 for 20 min. Normal goat serum (SL038-10 ml, Solarbio, China) was then used to block the tissues for 30 min. Next, the tissue on the slice was covered with Anti-vWF antibody (1:400, ab6994, Rabbit, Abcam, USA) and Anti-KDR antibody (1:200, ab9530, Mouse, Abcam, USA) overnight at 4°C. The next day, Goat Anti-Rabbit (FITC, 1:3000, ab6717, Abcam, USA) and Anti-Mouse (PE, 1:3000, ab7000, Abcam, USA) were combined with corresponding primary antibodies for 1 h. The nucleus of cells was stained with DAPI for 3 min. The numbers of cells positively expressing vWF and KDR in the stained tissues were counted by a Zeiss L LSM800 confocal microscope (Germany) at 200× magnification.

Flow cytometry

In this study, a FACSAria II flow cytometer (BD, USA) was used to count the number of EPCs in the cell suspension by identifying the fluorescent signals of KDR and CD34 positive expres-

Table 1. Primers for qRT-PCR

Genen	Forward primer (5'-3')	Reverse primer (5'-3')
NEAT1	GGCAGGTCTAGTTTGGGCAT	CCTCATCCCTCCCAGTACCA
miR-204-5p	GCCTGTCGTATCCAGTGCAA	GTCGTATCCAGTGCGTGTCG
U6	AAAGCAAATCATCGGACGACC	GTACAACACATTGTTTCCTCGGA
β-actin	ATTGGCAATGAGCGGTTC	GGATGCCACAGGACTCCA

sion. Cell suspension was first prepared with uncontaminated EPCs, and the cell density was adjusted to 1×10^6 cells/mL. Next, the EPC suspension was added with 0.5 μL of Anti-KDR antibody (0.5 mg/mL, ab9530, Mouse, Abcam, USA) and 0.5 μL of Anti-CD34 antibody (0.5 mg/mL, ab81289, Rabbit, Abcam, USA) for 1 h at room temperature. Then the cells were further combined with 1 μL of fluorescent-labeled secondary antibody (Anti-Mouse PE, 0.5 mg/mL, ab7000, Abcam, USA; Goat Anti-Rabbit FITC, 0.5 mg/mL, ab6717, Abcam, USA) for 30 min at room temperature. After washing with FACS buffer, EPCs were transferred to a flow cytometer to detect the fluorescent expressions of KDR and CD34.

Isolation and cultivation of endothelial progenitor cells (EPCs)

Three SD rats were deeply anesthetized and sacrificed under pentobarbital sodium anesthesia. After the rats were fixed and thoroughly disinfected, the left hind limb of the rats was cut off, and the femur and tibia were peeled off and placed in a sterile culture dish. Sterile surgical instruments were applied to cut off the epiphysis, and then the bone marrow cavity was washed with PBS. The collected bone marrow suspension was centrifuged using density gradient centrifugation for 5 min at 4°C at 1,600×g. The resulting pellet was re-suspended in PBS again. Afterwards, the suspension was mixed with the lymphocyte separation solution at the ratio of 1:1. After another round of centrifugation (15 min at 2,000×g, 4°C), the milky white intermediate layer of monocytes was then collected and washed. The cells were finally transferred to EGM-2 medium (CC-3162, Lonza, Switzerland) and cultured (at 37°C with 5% CO_2).

The primary cells were cultured for 3 days before passage. To identify the cells, the expressions of KDR and CD34 markers in the primary cells re-suspended in the culture medium were examined with a flow cytometer. The cell morphology was observed with a Leica microscope (DM1000, Germany) at 100× magnification on the 6th and 17th days of passage.

Double labeling method for identifying EPCs

The DiI-Ac-LDL/FITC-UEA-1 double labeling method was carried out on the tenth day of cell passage to identify the isolated EPCs. The adherent EPCs were first incubated with DiI-Ac-LDL reagent (4 μg/mL, FS1088-500UG, Fushen, China) in an environment at 37°C for 4 h. The cells were then washed with PBS for 5 min for a total of 3 times. Next, the cells were fixed with paraformaldehyde for 10 min. After that, FITC-UEA-1 reagent (10 μg/mL, FS1109-500UG, Fushen, China) was added to EPCs for 1-h incubation at room temperature. After the incubation, the staining results were observed with a Zeiss L LSM800 confocal microscope (Germany) at 200× magnification.

Quantitative real-time polymerase chain reaction (qRT-PCR)

Trizol (15596018, ThermoFisher, USA) was added to EPCs for RNA isolation, and chloroform (CP287, 9dingchem, China) and isopropanol (I112023, Aladdin, China) were added into EPCs in sequence to obtain RNA precipitation. The RNA concentration was measured using a ND-LITE-PR NanoDrop 2000 instrument produced by ThermoFisher (USA).

The K1621 kit (ThermoFisher) was applied for reverse transcription of RNA into cDNA. The synthesized cDNA and gene primer designed by Sangon (China) were mixed for the PCR under the following conditions: pre-denaturation at 95°C for 10 min, denaturation at 95°C for 15 seconds (s), annealing at 60°C for 1 min, for a total of 40 cycles. After the detection, the final results were obtained using the computer program by the $2^{-\Delta\Delta CT}$ method [18]. The sequences of primers to be tested were listed in **Table 1**.

MTT assay

In short, the EPC suspension was prepared by treatment with trypsin (S10032-100 g, Yuanye, China) and PBS. Two thousand EPCs were inoculated into the bottom of a 96-well plate. After 24 hours of incubation, 5 mg/mL MTT solution (E606334-0250, Sangon, China) was added into EPCs and fully mixed. Then the EPCs were

continuously incubated for 4 h at 37°C. 100 μL of Formazan Solubilization Solution in the kit as the reaction termination solution was added to the cells. Finally, the absorbance of cells at 570 nm was measured using a Molecular Devices (USA) SpectraMax i3x microplate reader.

Wound-healing assay

Horizontal lines at a space of 1 cm were drawn on the back of the 6-well plate. The EPC suspension prepared was transferred into 6-well plates at a density of 5×10^5 cells/well. The cells were then incubated overnight to continue the observation (37°C, 5% CO_2). Next, a pipette was used to draw a gap perpendicular to the previous line in the 6-well plate containing cells. The 6-well plate was then added with serum-free medium and further incubated for 24 h. Afterwards, cell migration was observed under a microscope at 100× magnification.

Tube formation assay

Matrigel stored at 4°C was first evenly spread on the bottom of a 96-well plate (50 μL/well). The 96-well plate was then transferred to a cell incubator and incubated for 30 min at 37°C. The transfected EPCs were collected and adjusted to a cell concentration of 2×10^5 cells/mL. Next, 100 μL of EPC suspension was added to the 96-well plate after incubation. The EPCs were continuously incubated for 4 h, and then observed under a Leica DM1000 microscope (Germany) the growth changes of the small tube structure at 100× magnification.

Enzyme-Linked ImmunoSorbent Assay (ELISA)

The EPC supernatant was collected to measure the content of vascular endothelial growth factor (VEGF) using a rat VEGF ELISA KIT (kt50063, MSKBIO, Germany). The supernatant and reagent were added to the bottom of the microtiter plate as required. After sealing the plate with a membrane, the microplate was placed at 37°C and incubated for 30 min. After solution preparation, the cells were washed, added with enzyme reagents for color development. When the reaction was terminated, the microplate was read by a microplate reader (SpectraMax i3x, Molecular Devices, USA) for the OD value (wavelength: 450 nm) of each well.

Western blot

The protein in the cell was separated into protein liquid by lysis (R0020-100 ml, Solarbio, China). In this study, the BCA method was employed to determine protein concentration [19]. Sodium dodecyl sulfate-polyacrylamide gel electrophoresis (SDS-PAGE) was used as a medium to promote protein transfer onto a 0.45-μm PVDF membrane (YA1701, Solarbio, China). The protein was further fixed on the membrane with a 5% BSA blocking solution (SW3015-100 mL, Solarbio, China). Then the primary antibody was added to incubate with the protein overnight to fully binding to the target protein (at 4°C). Subsequently, the proteins were treated with the secondary antibody for 1 h at room temperature. Protein bands were visualized using the luminescent fluid (PE0010) and gel imaging system (Tanon 2500, China) produced by Solarbio (China). The antibodies used in this experiment were as follows: Ang-1 (1:500, ab8451, Abcam, USA); phosphorylated Tyrosine kinase 2 (p-Tie-2, 1:500, ab192800, Abcam, USA); Tie-2 (1:1000, ab24859, Abcam, USA); phosphorylated extracellular regulated protein kinases (p-ERK, 1:1000, ab201015, Abcam, USA); ERK (1:1000, ab17942, Abcam, USA); B-actin (1:5000, ab8226, Abcam, USA); Goat Anti-Rabbit antibodies (1:5000, ab-205718, Abcam, USA) and Goat Anti-mouse antibodies (1:5000, ab150117, Abcam, USA).

Target prediction and verification

The targeting sequences of NEAT1 and miR-204-5p, and miR-204-5p and Ang-1 with 3'-untranslated regions (3'UTRs) were predicted on the starBase (http://starbase.sysu.edu.cn/index.php) and TargetScan databases (http://www.targetscan.org/). Dual-luciferase experiment was performed to further verify the results. The two sets of binding sequences were inserted into the PmirGLO vector (VT1439, YouBioChina) to synthesize the wild-type (NEAT1-WT, 5'-GUUUUCCGAGAACCAAAGGGAG-3'; Ang-1-WT, 5'-ACUGUCGAGUUUUGAAAAGGGAA-3') and mutant (NEAT1-mut, 5'-GUUUUCCGAGAACUGCUAACGG-3'; Ang-1-mut, 5'-ACUGUCGAGUUUUGACGGAUACA-3') reporter plasmids. Reporting plasmid/miR-204-5p mimic and mimic control (MC) were transfected into EPCs as required. A dual-luciferase reporter gene detection kit (D0010-100T, Solarbio,

China) was conducted to detect fluorescent activity of the reporter gene with a GloMax 20/20 detector (Promega, USA).

Statistical analysis

SPSS 21.0 (USA) was applied for data analysis. Student's two-tailed *t*-test was performed for comparing the differences between two groups, while one-way ANOVA followed by Tukey's test was employed for multi-group comparison. The data were expressed as mean ± standard deviation (SD). A P value of < 0.05 indicated that the difference was statistically significant.

Result

NEAT1 overexpression reduced aneurysm damage

A rat AAA model was set up to observe the effect of NEAT1 overexpression on abdominal aortic aneurysm *in vivo* and confirmed by pathological examination (H&E staining) on the abdominal aorta. The EPCs were identified by detecting the positive expression of the characteristic markers (vWF, KDR and CD34) of EPCs using immunofluorescence staining and flow cytometry. The results of pathological examination were shown in **Figure 1A**. The abdominal aorta of rats in the Sham group was normal. In the Model group, a thrombus was formed in the abdominal aorta and the media layer was peeled off. Leukocyte accumulation and elastin fibers in the ruptured aortic wall were visible in the media and adventitia. Vascular tissue lesions in the NC group were similar to those in the Model group. Compared with the Model group, the abdominal aortic was improved, the inflammatory cell infiltration in the middle layer of the blood vessel wall was significantly decreased, moreover, the content of aortic wall elastin was greatly increased in the NEAT1 group. We also determined the expression of NEAT1 in the tissues. The results showed that the AAA model suppressed the expression of NEAT1, while exogenous overexpression of NEAT1 (NEAT1 group) up-regulated the mRNA expression of NEAT1 (**Figure 1B**, P < 0.001).

Cells positively expressing vWF (green) and KDR (red) in vascular tissues were identified through immunofluorescence (**Figure 1B**). The number of vWF^+ and KDR^+ cells in aneurysm tissues in the Model group was significantly more than that in the Sham group, and overexpression of NEAT1 further increased the number of these cells in the aneurysm tissues.

Flow cytometry was performed to detect the expressions of EPC markers $CD34^+$ and KDR^+ in the peripheral blood of rats to identify the changes of EPCs in the peripheral blood. The data demonstrated that compared with the Sham group, the number of $CD34^+$ and KDR^+ positive cells in the peripheral blood of the Model group was significantly reduced (**Figure 1D-F**, P < 0.001). The intervention of overexpressed NEAT1 successfully increased the number of $CD34^+$ and KDR^+ positive cells in the serum of AAA rats (**Figure 1D-F**, P < 0.01). The above results revealed that NEAT1 overexpression could promote the formation of EPCs in model rats.

Endothelial progenitor cells were successfully isolated

We first observed the EPCs extracted from rat bone marrow with a microscope (**Figure 2A**). On the sixth day of the primary cell culture, we found that some cells were spindle-shaped, and some formed a string-like structure. On the 17th day, the cells exhibited paving stone-like appearance. The results of functional tests were shown in **Figure 2B** and **2C**, specifically, the cells were able to absorb DiI-ac-LDL and were bound by UEA on the cell membrane, at the same time, the cells were double positive for CD34 and KDR. These results proved that the cells we isolated and cultured were EPCs.

By regulating VEGF and Ang-1/ERK, NEAT1 significantly regulated the function of EPCs

Overexpressed or silenced NEAT1 was transfected into EPCs, and the transfection rate was determined by qRT-PCR. NEAT1 overexpression was found to significantly upregulate the expression of NEAT1, while knocking down NEAT1 resulted in the opposite effect (**Figure 3A**, P < 0.001). Then we examined the physiological function of EPCs, and found that NEAT1 overexpression could promote the viability, migration, and tube formation of EPCs, and increase the content of VEGF in EPCs (**Figure 3B-G**, P < 0.05). Further studies showed that the overexpressed NEAT1 significantly up-regulated the protein expressions of Ang-1, p-Tie-2 and p-ERK, whereas the expressions of Tie-2 and ERK did not change significantly (**Figure 4A-D**, P < 0.001). On the contrary, knocking

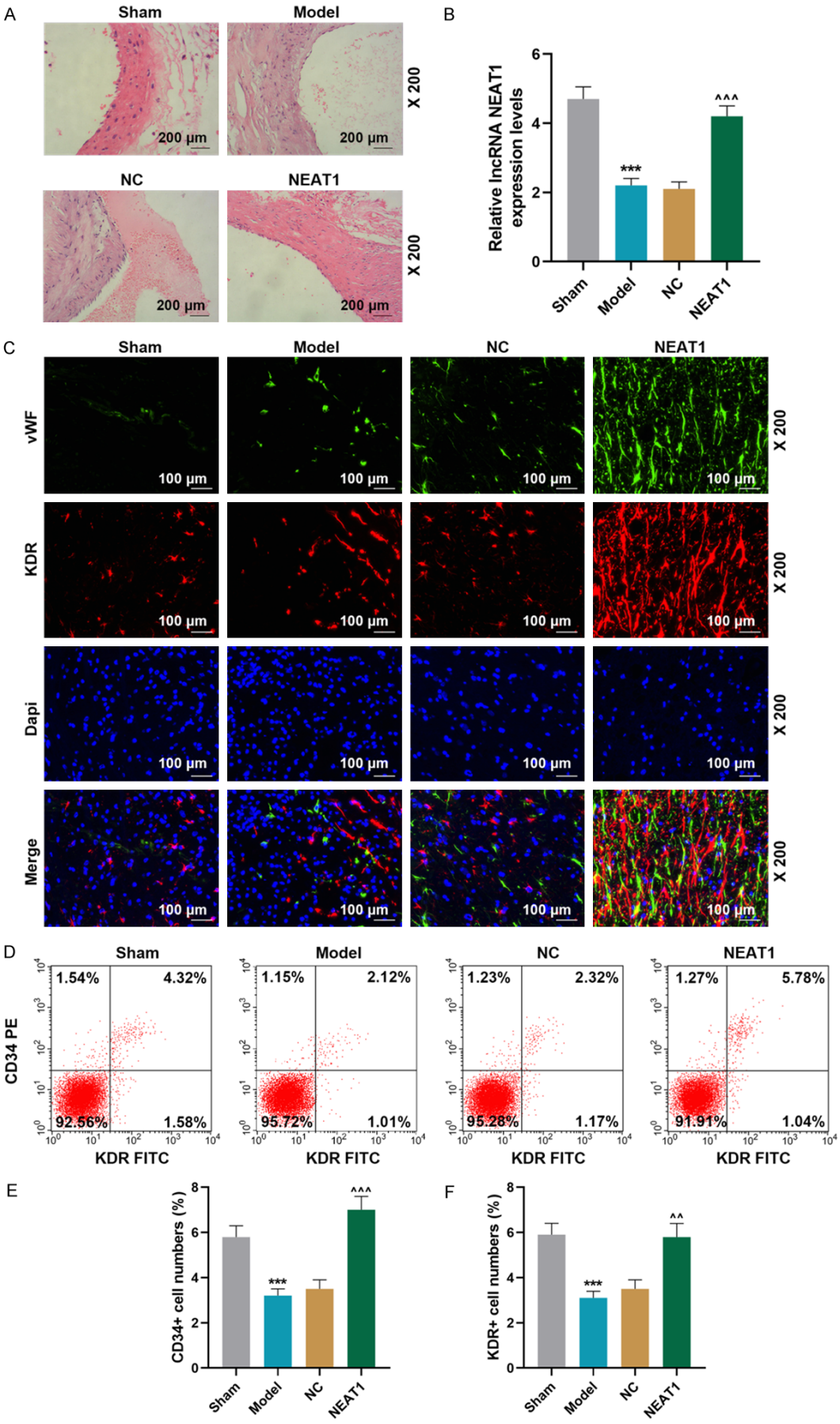
A
Sham
Model
NC
NEAT1
200 μm
X 200
B
Relative lncRNA NEAT1 expression levels
***
^^^
Sham
Model
NC
NEAT1
C
vWF
KDR
Dapi
Merge
100 μm
X 200
D
CD34 PE
KDR FITC
1.54%
4.32%
92.56%
1.58%
1.15%
2.12%
95.72%
1.01%
1.23%
2.32%
95.28%
1.17%
1.27%
5.78%
91.91%
1.04%
E
CD34+ cell numbers (%)
F
KDR+ cell numbers (%)
^^

Figure 1. The effect of NEAT1 overexpression on abdominal aortic aneurysm in the rats. A. The effect of NEAT1 overexpression on rat abdominal aortic aneurysms was observed by hematoxylin-eosin staining, at 200× magnification. B. The mRNA expression of NEAT1 in rat abdominal aorta was detected by qRT-PCR. β-actin was an internal reference. C. The effect of NEAT1 overexpression on the numbers of vWF^+ and KDR^+ cells in rat abdominal aortic aneurysms was observed by immunohistochemical staining, at 200× magnification. D-F. The effect of NEAT1 overexpression on the number of EPCs in rat abdominal aortic aneurysms was examined by flow cytometry. D and F. were the statistical analysis of the number of CD34 and KDR positive expression cells. All the experiments have been performed independently in triplicate. NEAT1: nuclear-enriched abundant transcript 1; vWF: von Willebrand Factor; KDR: kinase domain containing receptor.

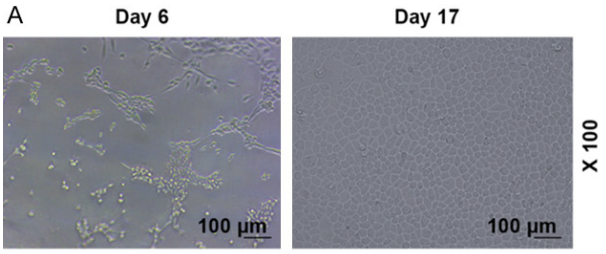

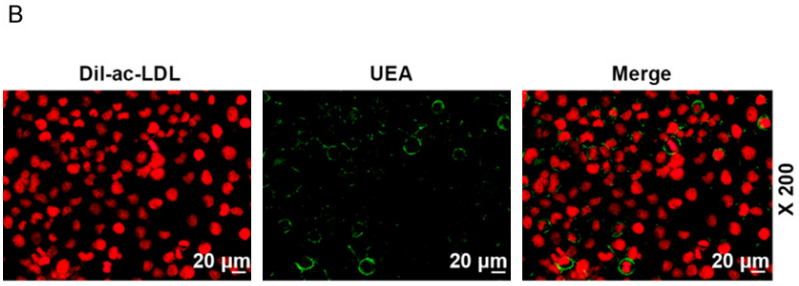

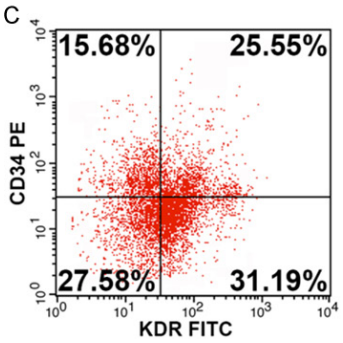

Figure 2. Isolation and identification of endothelial progenitor cells (EPCs). A. Cell morphology was observed under a microscope, at 100× magnification. B. The isolated and cultured cells were identified by Dil-ac-LDL staining, at 200× magnification. C. The isolated and cultured cells were identified by flow cytometry. All the experiments have been performed independently in triplicate.

down NEAT1 produced completely opposite regulatory effects on EPCs (**Figures 3B-G** and **4A-D**, $P < 0.05$). The above results showed that NEAT1 can activate VEGF and Ang-1/ERK axis, thereby promoting the basic functions of EPCs.

NEAT1 targeted miR-204-5p and inhibited miR-204-5p expression

We searched the miRNA target of NEAT1 on starBase and found that NEAT1 had targeted binding sequences for miR-204-5p (**Figure 4E**). Further verification experiments confirmed their targeting relationship because the fluorescence activity of the NEAT1 - WT + miR-204-5p mimic group was inhibited (**Figure 4F**, $P < 0.001$). At the same time, we also found that overexpression of NEAT1 could inhibit the mRNA expression of miR-204-5p in EPCs, whereas siNEAT1 up-regulated miR-204-5p expression (**Figure 4G**, $P < 0.001$).

MiR-204-5p mimic neutralized the regulation of EPCs caused by NEAT1 upregulation

To clarify the effects of NEAT1 and miR-204-5p on EPCs, NEAT1 and miR-204-5p were overexpressed and transfected into EPCs. MiR-204-5p mimic was found to up-regulate the expression of miR-204-5p, suppress the expression of NEAT1, inhibit the viability, migration, and tube formation of EPCs, and reduce the content of VEGF in EPCs (**Figure 5A-H**, $P < 0.01$). In addition, miR-204-5p mimic also significantly suppressed the protein expressions of Ang-1, p-Tie-2 and p-ERK, and reduced the ratios of p-Tie-2/Tie-2 and p-ERK/ERK (**Figure 6A-D**, $P < 0.001$). However, NEAT1 produced the opposite effects, and partially reversed the function of miR-204-5p (**Figures 5** and **6**, $P < 0.01$).

Ang-1 interfered with the effects of NEAT1 and miR-204-5p on Ang-1 expression and EPC characteristics

TargetScan predicted that Ang-1 was the targeted regulatory gene of miR-204-5p (**Figure 7A**), and dual-luciferase experiments showed that there was indeed a targeted regulatory relationship between the two (**Figure 7B**, $P < 0.001$). Through co-transfection of cells with Ang-1 and miR-204-5p, we found that silencing Ang-1 inhibited the expression of Ang-1, while

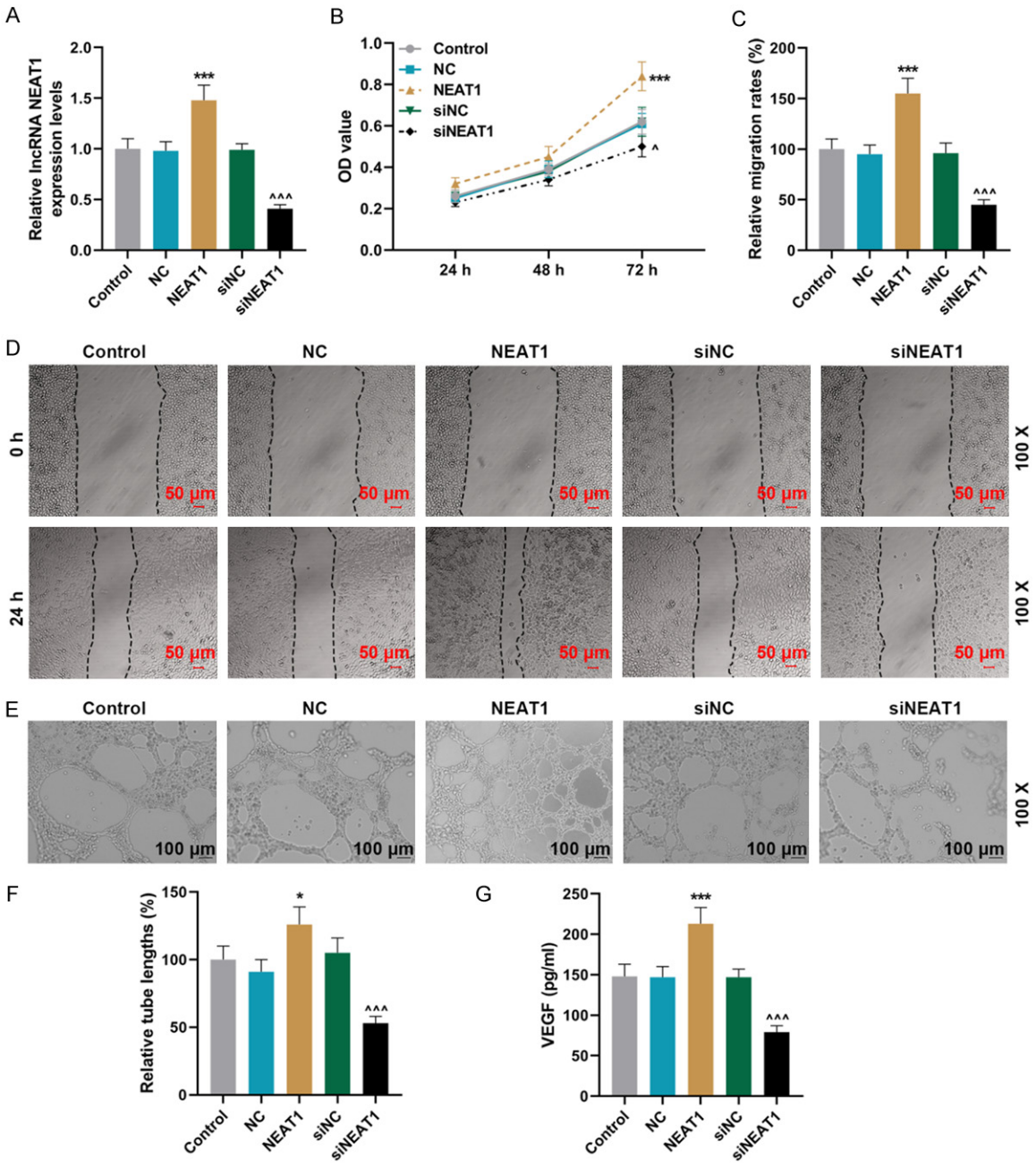

Figure 3. The effects of overexpression and silencing of NEAT1 on the viability, migration, tube formation of EPCs and VEGF content in EPCs. A. The transfection efficiency of overexpressed and silenced NEAT1 was analyzed by qRT-PCR. β-actin was used as an internal reference. B. The effects of overexpression and silencing of NEAT1 on the viability of EPCs were detected by MTT assay. C, D. The effects of overexpression and silencing of NEAT1 on the migration of EPCs were detected by wound-healing assay, at 100× magnification. E, F. The effects of overexpression and silencing of NEAT1 on EPC tube formation were detected by tube formation assay, at 100× magnification. G. The effects of overexpression and silencing of NEAT1 on VEGF content in EPCs were detected by Enzyme-Linked ImmunoSorbent Assay (ELISA). All experiments have been performed independently in triplicate. $^{*}P < 0.05$, $^{***}P < 0.001$ VS. NC; $^{\wedge}P < 0.05$, $^{\wedge\wedge\wedge}P < 0.001$ vs. siNC. QRT-PCR, Quantitative Real-Time Polymerase Chain Reaction; VEGF, Vascular endothelial growth factor; NC, negative Control; siNC, silent negative Control.

overexpressing Ang-1 produced the opposite effect (**Figure 7C-E**, $P < 0.001$). In the study of the characteristics of EPCs, it was observed that silencing Ang-1 reversed the protective

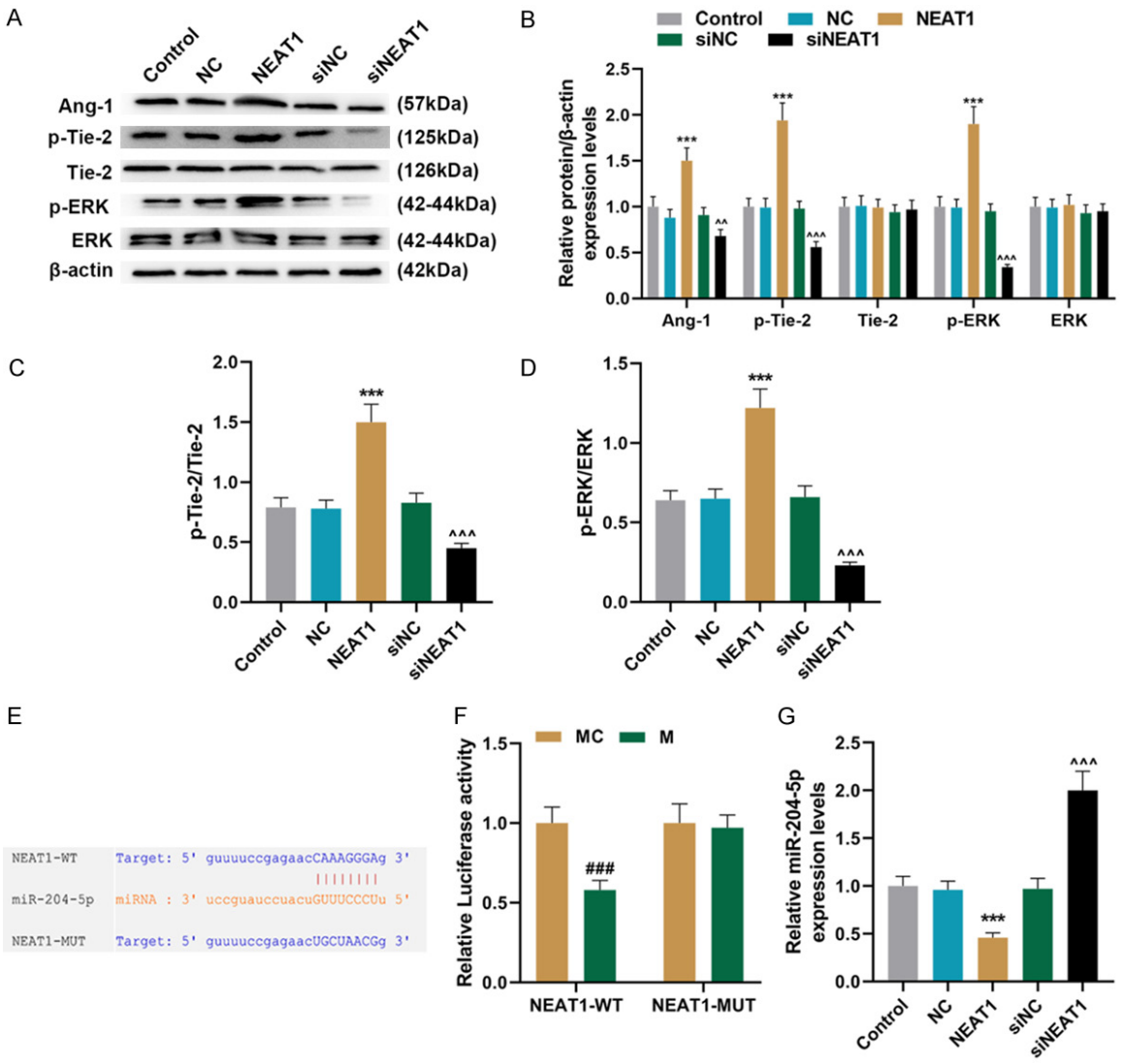

Figure 4. Overexpression and silencing of NEAT1 regulated the Ang-1/ERK pathway in EPCs, and NEAT1 targeted down-regulated miR-204-5p. A-D. Overexpression and silencing of NEAT1 regulated the protein expression of the Ang-1/ERK pathway in EPCs. β-actin was used as an internal reference. E. The targeted binding sites of NEAT1 and miR-204-5p were predicted by starBase (http://starbase.sysu.edu.cn/index.php). F. The targeted binding of NEAT1 and miR-204-5p was verified by dual-luciferase experiment. G. The effects of overexpression and silencing of NEAT1 on miR-204-5p expression were examined by qRT-PCR. U6 was used as an internal reference. All the experiments have been performed independently in triplicate. $^{***}P < 0.001$ vs. NC; $^{\wedge\wedge\wedge}P < 0.001$ vs. siNC; $^{\#\#\#}P < 0.001$ vs. MC. Ang-1, Angiopoietin-1; ERK, extracellular regulated protein kinases; MC: miR-204-5p mimic Control.

effect of overexpressed NEAT1 on EPC characteristics, including viability, migration and tube formation, and the expression of the Ang-1/p-ERK pathway (**Figures 7F-H** and **8**, $P < 0.05$). Furthermore, Ang-1 overexpression also reversed the inhibitory effect of NEAT1 mimic on EPCs (**Figures 7F-H** and **8**, $P < 0.01$).

Discussion

AAA is a common disease frequently occurring to middle-aged and elderly people. EPCs have the functions of repairing vascular injury and predicting the degree of early vascular injury [20]. Therefore, clarifying the action mechanism of EPCs in the treatment of AAA is of certain significance. As EPCs are abundant in the bone marrow, we therefore isolated and cultured EPCs from rat bone marrow. At the same time, EPCs lack the surface markers of endothelial cells and have no lumen-like structure, which imposes difficulty to distinguish EPCs only by morphology. CD34, vWF and KDR, which are currently widely used surface antigen mol-

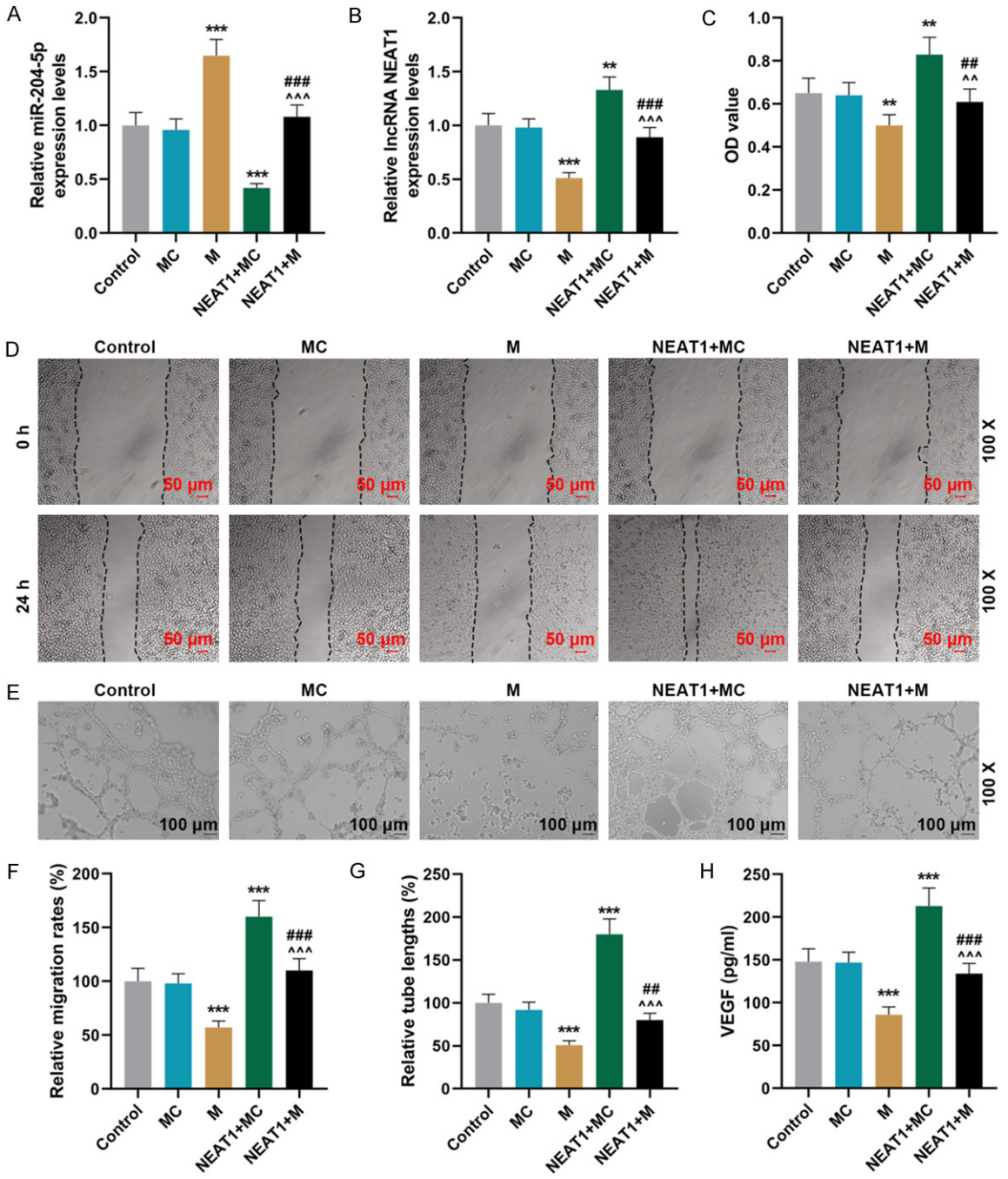

Figure 5. Effects of overexpressed NEAT1 and miR-204-5p on the expressions of NEAT1 and miR-204-5p, EPC viability, migration, and tube formation, VEGF content, and the Ang-1/ERK axis. A. The effects of overexpressed NEAT1 and miR-204-5p on miR-204-5p expression were analyzed by qRT-PCR. U6 was used as an internal reference. B. The effects of overexpressed NEAT1 and miR-204-5p on NEAT1 expression were analyzed by qRT-PCR. β-actin was used as an internal reference. C. The effects of overexpressed NEAT1 and miR-204-5p on the viability of EPCs were detected by MTT assay. D and F. The effects of overexpressed NEAT1 and miR-204-5p on the migration of EPCs were detected by wound-healing assay, at 100× magnification. E and G. The effects of overexpressions of NEAT1 and miR-204-5p on EPC tube formation were detected by tube formation assay, at 100× magnification. H. The effects of overexpressed NEAT1 and miR-204-5p on VEGF content in EPCs were detected by ELISA. All the experiments have been performed independently in triplicate. $^{**}P < 0.01$, $^{***}P < 0.001$ vs. MC; $^{\wedge\wedge}P < 0.01$, $^{\wedge\wedge\wedge}P < 0.001$ vs. NEAT1 + MC; $^{\#\#}P < 0.01$, $^{\#\#\#}P < 0.001$ vs. M. M: miR-204-5p mimic.

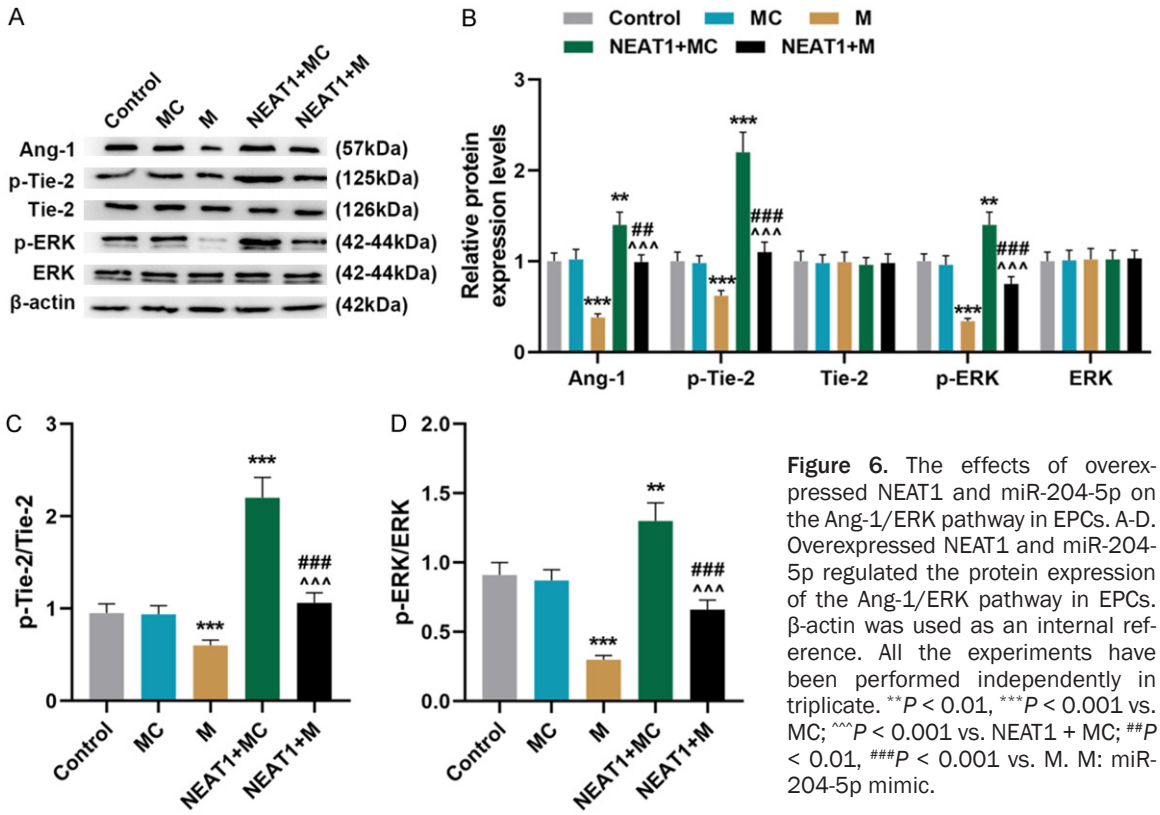

Figure 6. The effects of overexpressed NEAT1 and miR-204-5p on the Ang-1/ERK pathway in EPCs. A-D. Overexpressed NEAT1 and miR-204-5p regulated the protein expression of the Ang-1/ERK pathway in EPCs. β-actin was used as an internal reference. All the experiments have been performed independently in triplicate. $^{**}P < 0.01$, $^{***}P < 0.001$ vs. MC; $^{\wedge\wedge\wedge}P < 0.001$ vs. NEAT1 + MC; $^{\#\#}P < 0.01$, $^{\#\#\#}P < 0.001$ vs. M. M: miR-204-5p mimic.

ecules to distinguish EPCs [21], were confirmed as positive through microscopic observation in this study.

Further study proved that overexpression of NEAT1 can promote the repair of AAA. LncRNA NEAT1 is a newly discovered tumor-related gene [13] also critical for non-neoplastic diseases [22]. Zhang found that the loss of NEAT1 reduce the inflammatory response in mice with peritonitis and pneumonia, and prevents the activation of inflammatory bodies in macrophages [23]. An *et al.* [24] explained that neuronal lesions are usually accompanied by the abnormal expression of NEAT1. However, there are few reports on NEAT1 reducing vascular injury. We discovered for the first time that NEAT1 could enhance the physiological functions of EPCs and reduce the vascular damage caused by AAA, which was related to the activation of the Ang-1/ERK pathway induced by NEAT1.

The formation of neovascularization refers to the process of vascular endothelial cell proliferation and neovascularization under the joint action of various vascular growth factors [25], and among them, VEGF and Ang-1 are the most critical factors. VEGF is a potent mitogen highly selective to endothelial cells. Previous studies have suggested that VEGF can specifically act on vascular endothelial cells, and it can also induce the expressions of matrix metalloproteinases and collagenases, promote the degradation of extracellular matrix, and facilitate the migration of endothelial cells, thereby promoting the migration of endothelial cells and generation of new blood vessels [26, 27]. Ang-1 plays an important regulatory role between endothelium and endothelium-matrix, promotes the maturation of VEGF-induced immature blood vessels, maintains blood vessel structure, stabilizes endothelial cells, and inhibits its apoptosis, thus promoting endothelial cell growth [28]. Tie-2 is a common receptor of Ang-1 and Ang-2. Ang-1 cannot directly participate in the regulation of angiogenesis and stability, and it can also regulate the process by binding to Tie-2 receptor and promoting Tie-2 phosphorylation [29]. Ayumi also concluded that ERK activation is the key to the angiogenesis process [30]. Our results were similar to those reported by previous researchers, for

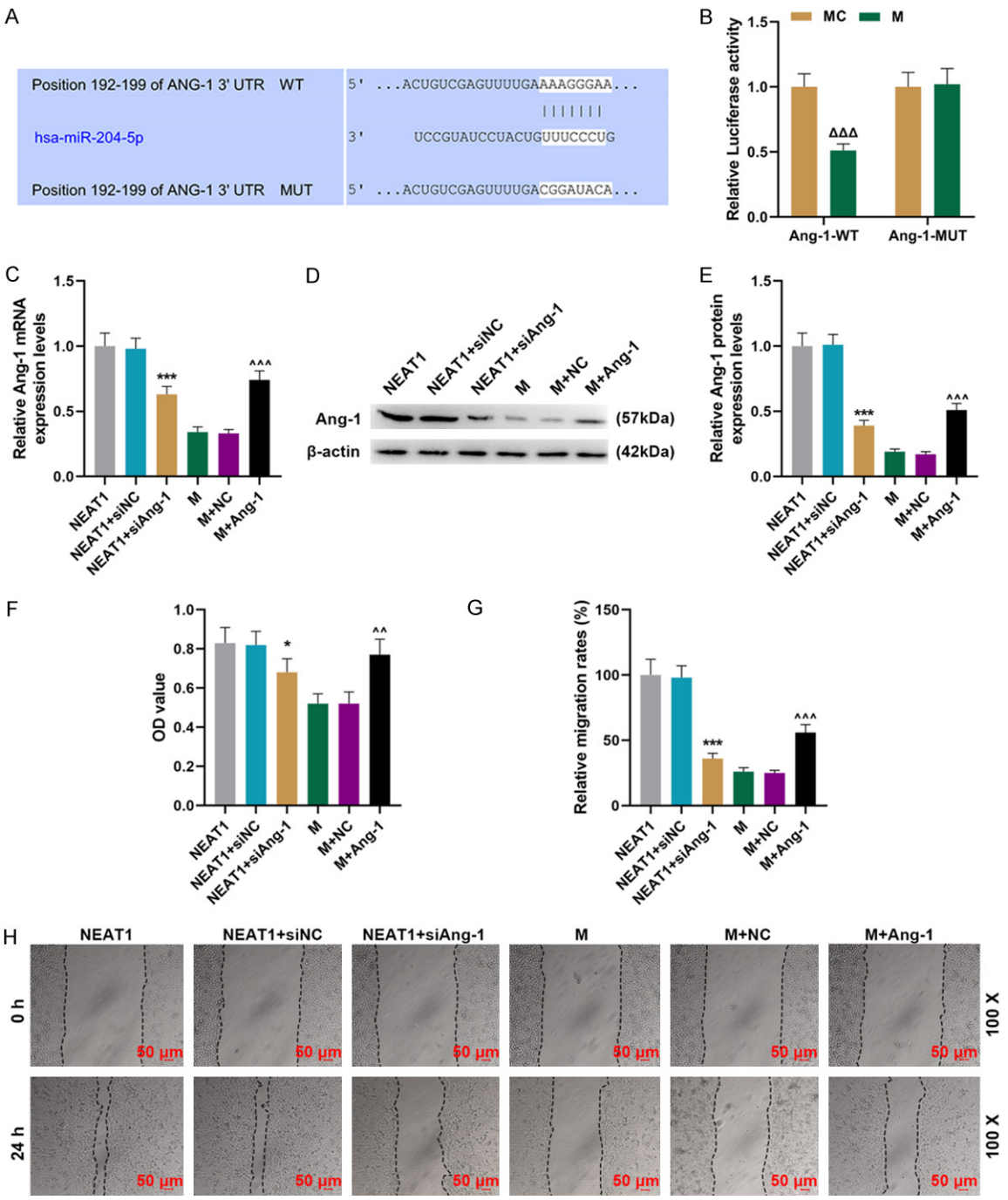

Figure 7. Effects of Ang-1, NEAT1 and miR-204-5p on Ang-1 expression, EPC viability and migration. A. The targeted binding sites of Ang-1 and miR-204-5p were predicted by TargetScan (http://www.targetscan.org/). B. The targeted binding of Ang-1 and miR-204-5p was verified by dual-luciferase experiment. C. The effects of Ang-1, NEAT1 and miR-204-5p on the mRNA expression of Ang-1 were analyzed by qRT-PCR. β-actin was used as an internal reference. D, E. The effects of Ang-1, NEAT1 and miR-204-5p on the protein expression of Ang-1 were analyzed by qRT-PCR. β-actin was used as an internal reference. F. The effects of Ang-1, NEAT1 and miR-204-5p on the viability of EPCs were detected by MTT assay. G, H. The effects of Ang-1, NEAT1 and miR-204-5p on the migration of EPCs were detected by wound-healing assay, at 100× magnification. All the experiments have been performed independently in triplicate. $^{\Delta\Delta\Delta}P < 0.001$ vs. MC; $^{*}P < 0.05$, $^{***}P < 0.001$ vs. NEAT1 + siNC; $^{\wedge\wedge}P < 0.01$, $^{\wedge\wedge\wedge}P < 0.001$ vs. M + NC.

example, Wang found that NEAT1 overexpression up-regulates VEGF in gliomas.

The mutual regulation of lncRNA and miRNA with a targeted relationship is the key mecha-

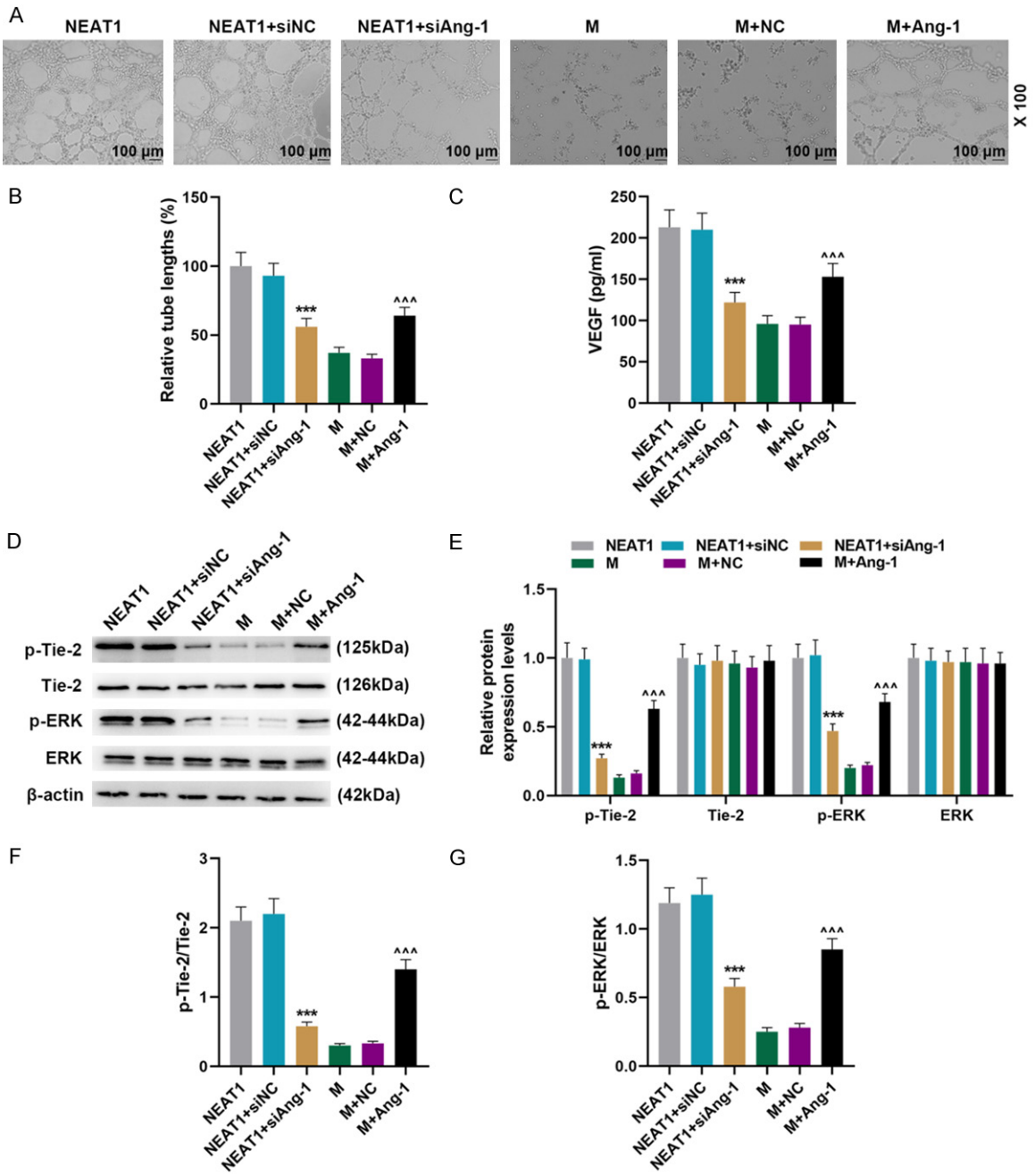

Figure 8. Effects of Ang-1, NEAT1 and miR-204-5p on EPC tube formation and the Tie/ERK pathway. A, B. The effects of Ang-1, NEAT1 and miR-204-5p on EPC tube formation were detected by tube formation assay, at 100× magnification. C. The effects of Ang-1, NEAT1 and miR-204-5p on the VEGF content in EPCs were detected by ELISA. D-G. Ang-1, NEAT1 and miR-204-5p regulated the protein expression of the Tie/ERK pathway in EPCs. β-actin was used as an internal reference. All the experiments have been performed in independent triplicate. $^{***}P < 0.001$ vs. NEAT1 + siNC; $^{\wedge\wedge\wedge}P < 0.001$ vs. M + NC.

nism for lncRNAs to exert its functions. This study found that miR-204-5p was targeted by NEAT1 and Ang-1. MiR-204-5p has a significantly low expression l in esophageal cancer and hepatocellular carcinoma, and this can inhibit the proliferation and metastasis of tumor cells by targeting different target genes [31, 32]. Moreover, miR-204-5p can prevent myoblast differentiation via reducing MEF2C and ERRγ expressions [33]. Furthermore, miR-

204-5p was identified to be related to breast cancer angiogenesis [34]. In our study, the up-regulation of miR-204-5p inhibited the viability, migration, tube formation of EPCs, and the expressions of angiogenesis-related factors.

In the current study, injection of the lentivirus NEAT1 overexpression vector via the tail vein significantly promoted the repair of AAA in rats, and increased the number of endothelial progenitor cells in the peripheral blood of rats. In *in vitro* experiments, we found that NEAT1 could up-regulate the expression of Ang-1 in EPCs through competitive binding and inhibiting miR-204-5p expression, thus effectively promoting the proliferation, migration and tube formation of EPCs. Our research provides reliable basic research data to the molecular targeted therapy for AAA.

Acknowledgements

This work was supported by the Key Research and Development Plan of Anhui Province [1804h08020280].

Disclosure of conflict of interest

None.

Address correspondence to: Youmin Pan, Department of Cardiovascular Surgery, Tongji Hospital, Tongji Medical College, Huazhong University of Science and Technology, No. 1095 Jiefang Avenue, Hankou, Wuhan 430030, Hubei Province, China. Tel: +86-027-83665390; E-mail: pyoumin_panym@163.com

References

[1] Nordon IM, Hinchliffe RJ, Loftus IM and Thompson MM. Pathophysiology and epidemiology of abdominal aortic aneurysms. Nat Rev Cardiol 2011; 8: 92-102.
[2] Legg JS and Legg LM. Abdominal aortic aneurysms. Radiol Technol 2016; 88: 145-163.
[3] Sakalihasan N, Limet R and Defawe OD. Abdominal aortic aneurysm. Lancet 2005; 365: 1577-1589.
[4] Kent KC. Clinical practice. Abdominal aortic aneurysms. N Engl J Med 2014; 371: 2101-2108.
[5] Wang YD, Liu ZJ, Ren J and Xiang MX. Pharmacological therapy of abdominal aortic aneurysm: an update. Curr Vasc Pharmacol 2018; 16: 114-124.
[6] Ullery BW, Hallett RL and Fleischmann D. Epidemiology and contemporary management of abdominal aortic aneurysms. Abdom Radiol (NY) 2018; 43: 1032-1043.
[7] Asahara T, Murohara T, Sullivan A, Silver M, van der Zee R, Li T, Witzenbichler B, Schatteman G and Isner JM. Isolation of putative progenitor endothelial cells for angiogenesis. Science 1997; 275: 964-967.
[8] Peters EB. Endothelial progenitor cells for the vascularization of engineered tissues. Tissue Eng Part B Rev 2018; 24: 1-24.
[9] Garikipati VNS and Kishore R. Endothelial progenitor cells: procedure for cell isolation and applications. Methods Mol Biol 2017; 1553: 85-89.
[10] Rana D, Kumar A and Sharma S. Endothelial progenitor cells as molecular targets in vascular senescence and repair. Curr Stem Cell Res Ther 2018; 13: 438-446.
[11] Skurikhin EG, Krupin VA, Pershina OV, Pan ES, Ermolaeva LA, Pakhomova AV, Rybalkina OY, Ermakova NN, Khmelevskaya ES, Vaizova OE, Zhukova MS, Pozdeeva AS, Skurikhina VE, Goldberg VE and Dygai AM. Endothelial progenitor cells and Notch-1 signaling as markers of alveolar endothelium regeneration in pulmonary emphysema. Bull Exp Biol Med 2018; 166: 201-206.
[12] Lee YT, Tan YJ and Oon CE. Molecular targeted therapy: treating cancer with specificity. Eur J Pharmacol 2018; 834: 188-196.
[13] Yu X, Li Z, Zheng H, Chan MT and Wu WK. NEAT1: a novel cancer-related long non-coding RNA. Cell Prolif 2017; 50: e12329.
[14] Klec C, Prinz F and Pichler M. Involvement of the long noncoding RNA NEAT1 in carcinogenesis. Mol Oncol 2019; 13: 46-60.
[15] Chen LL and Carmichael GG. Altered nuclear retention of mRNAs containing inverted repeats in human embryonic stem cells: functional role of a nuclear noncoding RNA. Mol Cell 2009; 35: 467-478.
[16] Ahmed ASI, Dong K, Liu J, Wen T, Yu L, Xu F, Kang X, Osman I, Hu G, Bunting KM, Crethers D, Gao H, Zhang W, Liu Y, Wen K, Agarwal G, Hirose T, Nakagawa S, Vazdarjanova A and Zhou J. Long noncoding RNA NEAT1 (nuclear paraspeckle assembly transcript 1) is critical for phenotypic switching of vascular smooth muscle cells. Proc Natl Acad Sci U S A 2018; 115: E8660-E8667.
[17] Tekin G, İsbir S, Şener G, Çevik Ö, Çetinel Ş, Derici oğlu O, Arsan S and Çobanoğlu A. The preventive and curative effects of melatonin against abdominal aortic aneurysm in rats. J Vasc Surg 2018; 67: 1546-1555.
[18] Schmittgen TD and Livak KJ. Analyzing real-time PCR data by the comparative C(T) method. Nat Protoc 2008; 3: 1101-1108.
[19] Jeong DE, Lee Y and Lee SV. Western blot analysis of C. elegans proteins. Methods Mol Biol 2018; 1742: 213-225.

[20] Ozkok A and Yildiz A. Endothelial progenitor cells and kidney diseases. Kidney Blood Press Res 2018; 43: 701-718.
[21] Flammer AJ, Gössl M, Widmer RJ, Reriani M, Lennon R, Loeffler D, Shonyo S, Simari RD, Lerman LO, Khosla S and Lerman A. Osteocalcin positive CD133+/CD34-/KDR+ progenitor cells as an independent marker for unstable atherosclerosis. Eur Heart J 2012; 33: 2963-2969.
[22] Prinz F, Kapeller A, Pichler M and Klec C. The implications of the long non-coding RNA NEAT1 in non-cancerous diseases. Int J Mol Sci 2019; 20: 627.
[23] Zhang P, Cao L, Zhou R, Yang X and Wu M. The lncRNA Neat1 promotes activation of inflammasomes in macrophages. Nat Commun 2019; 10: 1495.
[24] An H, Williams NG and Shelkovnikova TA. NEAT1 and paraspeckles in neurodegenerative diseases: a missing lnc found? Noncoding RNA Res 2018; 3: 243-252.
[25] Siveen KS, Prabhu K, Krishnankutty R, Kuttikrishnan S, Tsakou M, Alali FQ, Dermime S, Mohammad RM and Uddin S. Vascular endothelial growth factor (VEGF) signaling in tumour vascularization: potential and challenges. Curr Vasc Pharmacol 2017; 15: 339-351.
[26] Kang DH and Johnson RJ. Vascular endothelial growth factor: a new player in the pathogenesis of renal fibrosis. Curr Opin Nephrol Hypertens 2003; 12: 43-49.
[27] Ferrara N, Gerber HP and LeCouter J. The biology of VEGF and its receptors. Nat Med 2003; 9: 669-676.
[28] Machado MSR, Bertagnolli TV, Veiga ECA, Ferreira CJH, Duarte G, Machado JSR and Carvalho R. Role of plasma PlGF, PDGF-AA, ANG-1, ANG-2, and the ANG-1/ANG-2 ratio as predictors of preeclampsia in a cohort of pregnant women. Pregnancy Hypertens 2019; 16: 105-111.
[29] Nagasawa-Masuda A and Terai K. ERK activation in endothelial cells is a novel marker during neovasculogenesis. Genes Cells 2016; 21: 1164-1175.
[30] Wang C, Chen Y, Wang Y, Liu X, Liu Y, Li Y, Chen H, Fan C, Wu D and Yang J. Inhibition of COX-2, mPGES-1 and CYP4A by isoliquiritigenin blocks the angiogenic Akt signaling in glioma through ceRNA effect of miR-194-5p and lncRNA NEAT1. J Exp Clin Cancer Res 2019; 38: 371.
[31] Tang J, Li Z, Zhu Q, Wen W, Wang J, Xu J, Wu W, Zhu Y, Xu H and Chen L. miR-204-5p regulates cell proliferation, invasion, and apoptosis by targeting IL-11 in esophageal squamous cell carcinoma. J Cell Physiol 2020; 235: 3043-3055.
[32] Chu Y, Jiang M, Du F, Chen D, Ye T, Xu B, Li X, Wang W, Qiu Z, Liu H, Nie Y, Liang J and Fan D. miR-204-5p suppresses hepatocellular cancer proliferation by regulating homeoprotein SIX1 expression. FEBS Open Bio 2018; 8: 189-200.
[33] Sun W, Qin R, Qin R, Wang R, Ding D, Yu Z, Liu Y, Hong R, Cheng Z and Wang Y. Sam68 promotes invasion, migration, and proliferation of fibroblast-like synoviocytes by enhancing the NF-κB/P65 pathway in rheumatoid arthritis. Inflammation 2018; 41: 1661-1670.
[34] Chen X, Mangala LS, Mooberry L, Bayraktar E, Dasari SK, Ma S, Ivan C, Court KA, Rodriguez-Aguayo C, Bayraktar R, Raut S, Sabnis N, Kong X, Yang X, Lopez-Berestein G, Lacko AG and Sood AK. Identifying and targeting angiogenesis-related microRNAs in ovarian cancer. Oncogene 2019; 38: 6095-6108.